On the Simple Complexity of Carbon Monoxide on Oxide Surfaces: Facet-Specific Donation and Backdonation Effects Revealed on TiO2 Anatase Nanoparticles

Chiara Deiana, Ettore Fois, Gianmario Martra, Stephanie Narbey, Francesco Pellegrino, and Gloria Tabacchi. On the Simple Complexity of Carbon Monoxide on Oxide Surfaces: Facet-Specific Donation and Backdonation Effects Revealed on TiO2 Anatase Nanoparticles. CHEMPHYSCHEM. 17 (13) pp: 1956-1960.
DOI: 10.1002/cphc.201600284

On the Simple Complexity of Carbon Monoxide on Oxide Surfaces: Facet-Specific Donation and Backdonation Effects Revealed on TiO_2 Anatase Nanoparticles

Dr. Chiara Deiana,

Department of Chemistry and NIS Centre, University of Turin, Torino, Italy

Prof. Dr. Ettore Fois,

Department of Science and High Technology, University of Insubria and INSTM, Como, Italy

Prof. Dr. Gianmario Martra,

E-mail address: gianmario.martra@unito.it

Department of Chemistry and NIS Centre, University of Turin, Torino, Italy

Dr. Stéphanie Narbey,

Solaronix SA, Aubonne, Switzerland

Dr. Francesco Pellegrino,

Department of Chemistry and NIS Centre, University of Turin, Torino, Italy

Dr. Gloria Tabacchi

E-mail address: gloria.tabacchi@uninsubria.it

Department of Science and High Technology, University of Insubria and INSTM, Como, Italy

Abstract

Atomic-scale relationships between the structure of TiO_2 surfaces and the physicochemical properties of surface sites, functional for titania-based applications, can be obtained from IR spectroscopy by using carbon monoxide (CO) as a molecular probe. In the literature, it is reported that strongly unsaturated cationic Ti sites (Lewis acid), which are important for reactivity, should cause a large upshift of the CO stretching frequency. By using IR spectroscopy of CO on TiO_2 nanomaterials and theoretical analyses, here this model is challenged. It is shown that the stretching frequency of adsorbed CO results from a facet-dependent and synergic CO–surface donation (upshift) - surface–CO backdonation (downshift) mechanism. These results imply that the interaction of adsorbed molecules with the Ti centers is tuned by the surface oxygen atoms of the first coordination sphere, which play an active role as indirect electron density donors (Lewis base).

Titania (TiO_2) is among the most studied semiconducting materials due to its importance for sustainable processes with applications in the energy/power, healthcare/medical, engineering and consumer goods industries.[1] These processes take place at the surfaces of nanostructured TiO_2 films or nanoparticles and involve a multiplicity of chemical events dictated not only by the nature, concentration and spatial (de)localization of defects, but also, at a deeper level, by the type and heterogeneity of the exposed surfaces.[1] Whereas surface structures down to monoatomic-height step edges can be investigated by using microscopy, for example, scanning tunneling microscopy, in single-crystal TiO_2 materials,[2, 3] the fine surface details of nanoparticles still remain elusive. This is the domain of molecular probes: species whose spectroscopic behavior is shaped by the nature, local structure and the electronic states of the adsorbing sites. By harnessing this sensitivity, IR spectroscopy experiments might catch a fleeting glimpse of surface chemistry. For example, the extent of bond weakening deduced for the probe from IR spectroscopy data is normally correlated with the ability of the surface sites to perturb electronic states and initiate activation of the adsorbates.[4] As recognized from the first seminal findings[5] to recent advances,[6] carbon monoxide (CO) is among the most informative probes, owing to the high sensitivity of its internal stretching mode frequency (νCO) to interactions with the surface sites. This is due to its quite unique electronic structure (Figure 1), which enables CO to act simultaneously as a donor and an acceptor of electron density. On this basis, CO–surface site interactions have been traditionally classified as: 1) electrostatic interactions, 2) electron density donation from the highest occupied molecular orbital (HOMO) of CO (5σ), and 3) backdonation of electron density from the metallic center to the lowest unoccupied molecular orbitals (LUMO) of CO (2π*).[7, 8a, 8b] Even on regular surfaces, these mechanisms are simultaneously active, deeply interlaced with each other and difficult to disentangle from the interactions between adsorbed molecules. Nevertheless, there is a consensus on the predominance of mechanisms 1 and 2 over mechanism 3[9] in the absorption of CO on alkali metal and alkaline-earth metal oxides. This predominance was also demonstrated for Ti^{4+} sites in (110) rutile TiO_2,[8c, 10] and recently, even in stoichiometric and nonstoichiometric (101) surfaces of anatase TiO_2.[6b] As a result, CO is generally regarded as the probe-of-choice for investigating both the relative polarizing power/Lewis acidity and the structure of cationic surface sites: the higher the wavenumber of the adsorbed CO, the higher the coordinative unsaturation of the site.[11]

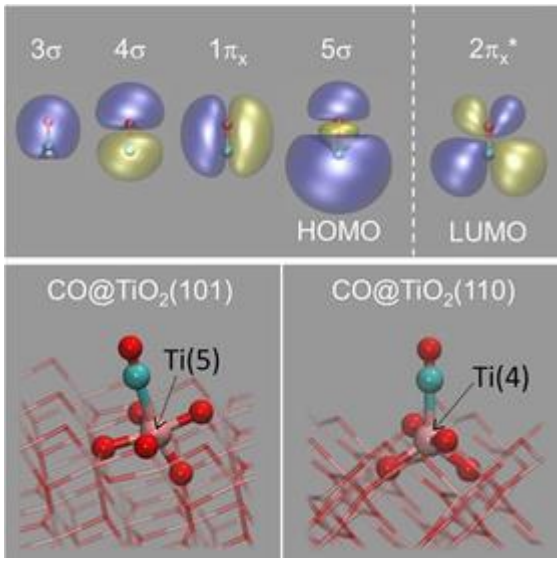

Figure 1.

Top: The electronic structure of CO. Left to right, with increasing energy: the occupied orbitals 3σ, 4σ, $1\pi_x$, and 5σ (HOMO), and the $2\pi_x$* LUMO. Only the *x* orbital of the 1π and 2π* pairs of degenerate states is shown. Positive lobes: blue, negative: yellow. Bottom: Optimized structures for the adsorption of CO on a Ti(5) site of the anatase (101) surface (left), and a Ti(4) site of the anatase (110) surface (right). CO, the Ti site, and its coordination environment are shown in ball-and-stick. Atom colors: C=cyan; O=red; Ti=pink.

This criterion is based on sound reasoning: a higher degree of unsaturation implies stronger polarizing power and/or Lewis acidity of the site, and, in the latter case, a greater withdrawal of electron density from the probe. As the CO HOMO has antibonding character (Figure 1, top), interaction with surface cations should cause a strengthening of the C−O bond, experimentally detectable by an upshift of the CO stretching band. By induction, this argument, originally put forward for insulating materials (e.g., MgO,[12, 13] Al_2O_3[14]), has been extended to semiconductor oxides of group 4 transition metals,[15] TiO_2 included, and the concept that higher *ν*CO wavenumbers are associated to strongly unsaturated and generally more reactive Ti centers, for example tetracoordinated [Ti(4)] rather than pentacoordinated [Ti(5)] sites, has been established over the years.[6, 9, 11, 16, 17] Herein, we show that exactly the opposite occurs at the (101) and (110) surfaces of anatase and we draw attention to a too-often overlooked aspect of TiO_2 materials: the oxygen atoms.[18]

To determine the *ν*CO values associated to Ti(5) and Ti(4) sites, we performed IR spectroscopic experiments on three types of fully oxidized anatase TiO_2 nanoparticles (Figures S1–S4 in the Supporting Information) containing different relative proportions of (101) and (110) facets, which expose Ti(5) and Ti(4) sites respectively (Figure 1 and Figure S5). Adsorbate–adsorbate interactions are both dynamic and static in nature and introduce additional factors affecting the frequency of adsorbed CO molecules.[9, 19] Dynamic lateral interactions are due to the coupling between the vibrating dipoles of the adsorbed molecules, and result in an upshift of *ν*CO with respect to the singleton frequency. By contrast, static interactions contain direct (due to the electrostatic interactions of the static dipoles) and indirect (interactions involving the surface) contributions, both of which result in a decrease of *ν*CO with respect to the singleton frequency. For CO adsorbed on oxides, static interactions overwhelmingly prevail over the dynamic ones, and a *ν*CO downshift occurs with increased CO coverage.[19] Adsorbate–adsorbate interactions depend on the distance between adsorbing sites, and in this study they should be weaker (and the downshift

smaller) at (110) facets compared to (101) facets because of the greater distance between Ti sites (5.46 vs. 3.80 Å respectively). To avoid these additional contributions to *ν*CO, we decreased the CO content of each sample from full coverage (θ=1) to a low coverage regime ($\theta \rightarrow 0$), at which the CO site interactions largely prevail over the CO–CO interactions. The first sample, hydrothermally (HT) prepared, consists of anatase TiO_2 nanoparticles with a well-defined truncated bipyramid shape, mainly limited by flat (101) surfaces exposing Ti(5) centers.[20] Accordingly, the IR spectrum for θ=1 shows only one sharp band centered at 2178 cm^{-1} (Figure 2, left, curve a), which gradually shifts to 2188 cm^{-1} with a progressive broadening if the coverage is decreased (Figure 2, left, curves a to k), owing to the decrease of CO–CO interactions.

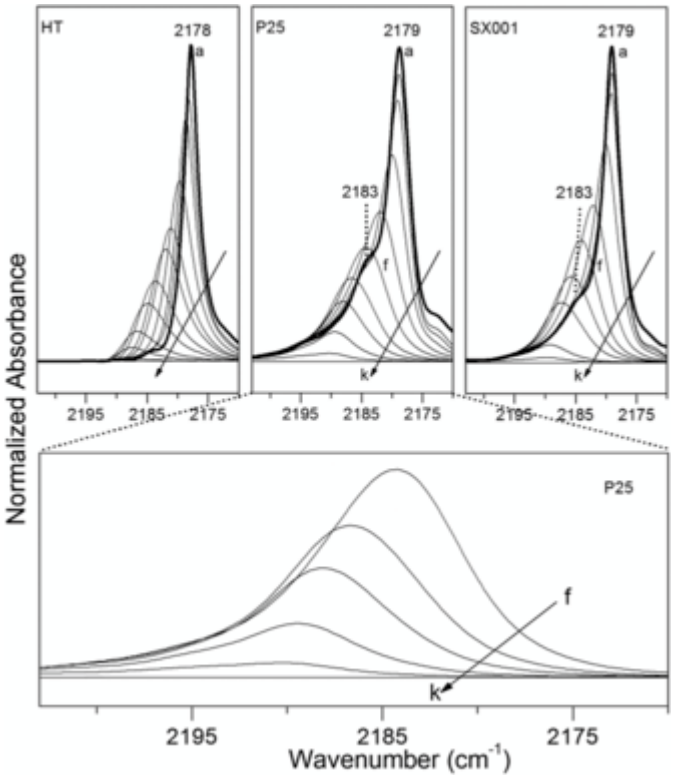

Figure 2.

IR spectra of CO adsorbed at 100 K (decreasing coverage in the sense of lettering) on HT (left), P25 (center) and SX001 (right) outgassed at 873 K. Bottom: zoomed-in view of IR spectra at low CO coverage on P25.

The spectrum of TiO_2 P25—a anatase/rutile mixture (≈80:20 *w*/*w*) considered a benchmark for heterogeneous photocatalytic processes—at high CO coverage (Figure 2, center panel, curve a) exhibits a main peak at 2179 cm^{-1} due to adsorbed CO on anatase (101) facets, and a partially resolved shoulder at 2183 cm^{-1}, due to CO on anatase (110) facets.[20] The same was observed for CO on SX001 (by Solaronix), a pure TiO_2 anatase powder (see the Supporting Information and Figure 2, right panel, curve a). The strong similarity between data obtained for P25 and SX001 confirms that the *ν*CO bands observed for P25 in this range are due only to CO adsorbed on the main anatase fraction of this material. By decreasing the CO coverage, the peak at 2179 cm^{-1} follows the same evolution observed for HT TiO_2, whereas the component at 2183 cm^{-1} is almost stable at the early stages of desorption (Figure 2, center and right panels, curves a–c), then gradually shifts to higher frequencies. Therefore, the signal due to CO on (110) facets, which is less affected by the decrease of the CO–CO interactions, is upshifted to a lower extent compared to the main peak. Interestingly, this trend continues upon further decrease of the CO coverage and the signals

overlap with each other (Figure 2, bottom panel). Because results obtained for HT TiO_2 provide evidence of CO left adsorbed on TiO_2 (101) facets in this low CO pressure regime, this behavior suggests that in the absence of adsorbate–adsorbate interactions, CO on (101) and (110) facets seems to exhibit similar internal stretching frequencies. These results are difficult to accommodate into the accepted model, which predicts that a higher degree of unsaturation [Ti(4) on (110) vs. Ti(5) on (101)] should produce a higher νCO upshift.[11]

To rationalize these findings, we modeled CO adsorption on regular (101) and (110) anatase surfaces at the $\theta \rightarrow 0$ limit by DFT calculations on periodic slab models, an approach already successful for the $\theta=1$ regime[20, 21] (see Section 2.1 of the Supporting Information). Two different adsorption geometries were found: whereas CO at the (101) surface saturates a Ti(5) center in a pseudo-octahedral environment, CO is bound to a Ti(4) site of the (110) surface in a trigonal-bipyramidal geometry, with the C atom on the bipyramid base and the CO axis almost perpendicular to the surface (Figure 1, bottom).

The data in Table 1 show that the binding energy is greater, the Ti−C distance is shorter and the separation of the C atom from the closest surface O atoms is also much shorter for CO at the Ti(4) sites of TiO_2(110). Hence, the Ti(4) sites interact more strongly than the Ti(5) sites with CO; this suggests a stronger Lewis acidity which, according to the generally accepted model, should be accompanied by a higher CO stretching frequency.[6h, 11, 17] Instead, in keeping with the trend outlined experimentally, at the $\theta \rightarrow 0$ limit we obtain for Ti(4) a νCO value lower than for Ti(5), and even a slightly longer C−O bond.

Table 1. Distance, binding energy (BE) and CO frequency, νCO.

	Ti_c[a]	**BE [kJ mol^{-1}]**	**Ti−C [Å]**	**C−O [Å]**	**νCO[b] [cm^{-1}]**	**Ti−O[c] [Å]**	**C−O_S[d] [Å]**
(101)	5	38.5	2.345	1.129	2196.2	1.854 1.871 1.975 1.975 2.013	2.835 2.856 2.856 3.024
(110)	4	50.2	2.249	1.130	2187.6	1.830 1.830 1.885 1.892	2.646 2.777

1. [a] Coordination of the Ti center. [b] Scaled values (f=1.011754, see the Supporting Information). [c] Coordination distances of the Ti site. [d] O_S: surface O atoms closest to C.

To shed more light, we inspected the electronic structure of the two systems. The density of states (DOS) projected on the C≡O atoms (Figure 3 a and b) shows a major stabilization of the CO HOMO upon adsorption. At the (101) surface, the 5σ orbital is split in two main peaks, indicating mixing of the CO HOMO with the TiO_2(101) states and a delocalized CO surface σ-bonding (Figure 3 c). Conversely, for CO at the (110) surface, the sharp 5σ peak and its greater stabilization compared to TiO_2(101) are evidence of a localized interaction with the Ti(4) site (Figure 3 d), and a stronger σ-donation to the empty d states of Ti, as confirmed by the more pronounced electron density accumulation at the Ti−C bond (Figure 4 d). Therefore, binding of CO to Ti(4) causes, compared to Ti(5), a greater depopulation of the CO HOMO, a stronger Ti−C bond, and a lower CO stretching frequency, which remains unexplained.

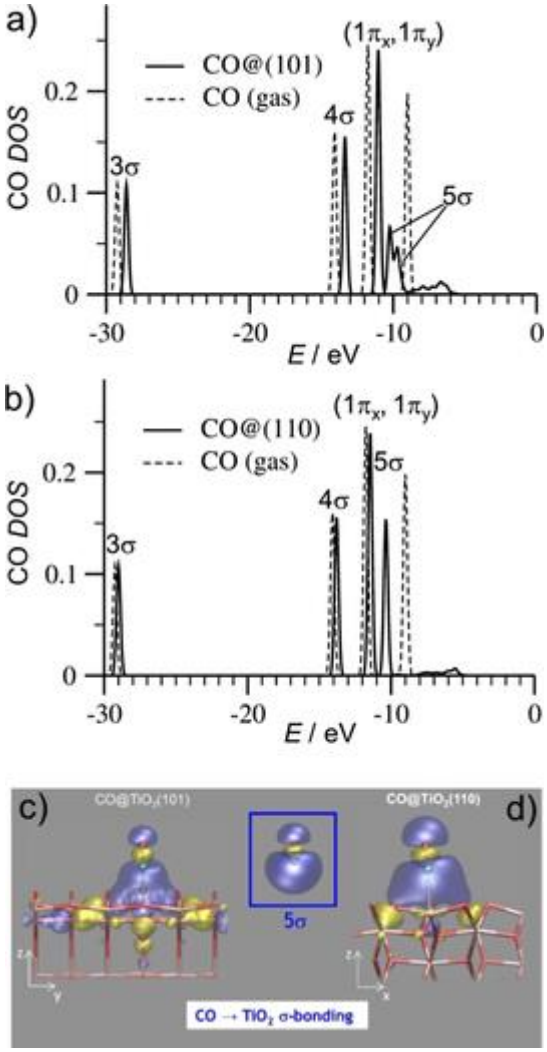

Figure 3.

CO density of states for a) CO@TiO_2(101) and b) CO@TiO_2(110); the DOS of gas-phase CO is also shown. The orbitals of CO@TiO_2(101) (c) and CO@TiO_2(110) (d), representing σ-bonding from the 5σ state of CO (inset) to the surface. Further data on the electronic structure analysis are in Section 2.2 of the Supporting Information. Positive lobes: blue, negative: yellow. Atom colors as in Figure 1.

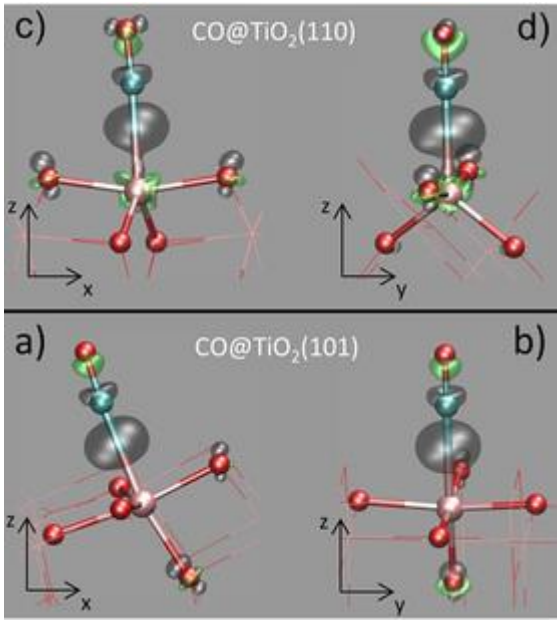

Figure 4.

Bonding charge density $\Delta\rho$ on the *xz* (left) and *yz* (right) planes. Charge accumulation regions=grey, depletion regions=green. $\Delta\rho$ (see for example, Ref. [8a] and [22], and Section 2.2.2 of the Supporting Information) is the change in electronic charge upon bringing CO to the surface (see also the contour plots in Figure S15). Results were validated with the hybrid functional PBE0 (Figure S16).

However, Figure 4 also reveals that, upon adsorption at the Ti(4) site of TiO_2(110), the electron density of CO increases on top of the O atom, indicating that antibonding orbitals of CO have been populated. To uncover these orbitals, we retrieved their fingerprints on the electronic states of the surface-molecule moieties (Figure 5 a–d). In the (101) case, although the state shown in Figure 5 a is reminiscent of the $2\pi_y$* orbital of CO, the state in Figure 5 b has bonding character with respect to the C−O bond and cannot be assigned to $2\pi_x$*. Indeed, very few states of the CO@TiO_2(101) system are C−O antibonding (Figure 5 e), which is consistent with the results reported in Ref. [6b]. In contrast, for CO at (110), the states shown in Figure 5 c and d both have a nodal plane perpendicular to the C−O axis, giving antibonding contributions to the C−O bond, and can be therefore traced to the $2\pi_y$* and $2\pi_x$* LUMO of CO, respectively. States such those shown in Figure 5 c and d are important fractions of the CO DOS for E>−9 eV and the dominant contribution at −7.5 eV (Figure 5 f).

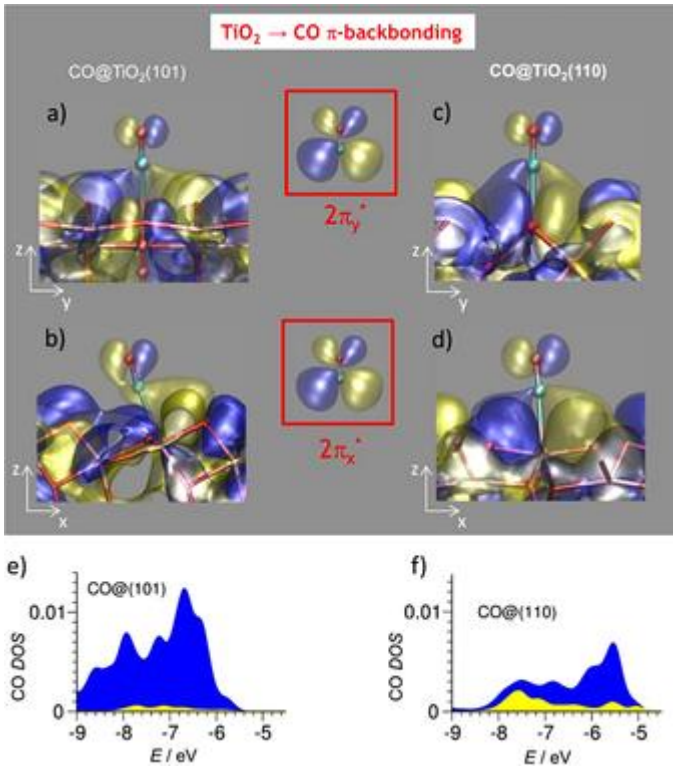

Figure 5.

Orbitals showing the surface–CO π-interactions. For CO@TiO_2(101), only $2\pi_y$*-backbonding is present (a); state b) has C−O bonding character. For CO@TiO_2(110), the orbitals shown in c) and d) represent π-backbonding from the TiO_2(110) valence band levels (composed by O 2p states) to the $2\pi_y$* and $2\pi_x$* LUMO of CO (inset), respectively. Positive lobes: blue, negative: yellow. Atom colors are as in Figure 1. Bottom: Enlarged view of the CO DOS of Figure 3 a and b for *E*>-9 eV, showing the total contribution of the states representative of π-backbonding (yellow) to the CO DOS (blue).

These data reveal that a donation–backdonation mechanism dominated by σ-bonding is operative in the adsorption of CO on TiO_2 surfaces. Both σ and π channels are more effective if CO is bound to Ti(4) sites at (110) facets compared to Ti(5) sites at (101) facets. Were σ-bonding the only contribution, the higher Lewis acidity of Ti(4) would result in a major strengthening of the C−O bond. However, backdonation from the TiO_2 valence band partially fills the CO LUMO. Such a bond-weakening effect is much greater for Ti(4) sites at (110) facets, because CO is oriented perpendicular to the surface and is close enough to the oxygen anions of the Ti(4) coordination sphere. Owing to this adsorption geometry, both $2\pi_x$* and $2\pi_y$* orbitals of CO are suitably oriented and well positioned for accepting electron density from TiO_2 (110) oxygen anions.

Hence, the surprisingly lower *ν*CO value found for the more unsaturated Ti(4) site results from a spectroscopic redshifting process due to surface CO backdonation, which is much stronger at the (110) surface compared to the (101) surface.

This process is inherently different from the standard backdonation that is typical of transition metals and metal cations with d electrons of suitable energy (Blyholder model).[7] In the present case, π-donation does not occur from the adsorbent Ti site (a d^0 cation), but from the surface oxygen anions of its coordination environment, which are not directly bonded to CO (Scheme 1). Furthermore, this new type of backdonation, here evidenced for the first time, is promoted by the Lewis acidity of the site through a strong Ti−C bond, which draws the molecule close to the surface

oxygen anions (see Scheme 1), but is ruled by the structure and electronic states (band structure) of the specific facet, which determine the adsorption geometry. Therefore, donation/backdonation—and also Lewis acidity/reactivity—should be regarded as surface properties rather than as properties of local sites. In a broader perspective, this mechanism could be a general aspect of molecule–surface interactions in d^0-metal oxides, which might provide insight to other phenomena, such as the charge density increase reported for the O atom of CO on TiO_2-B (100) surfaces.[23]

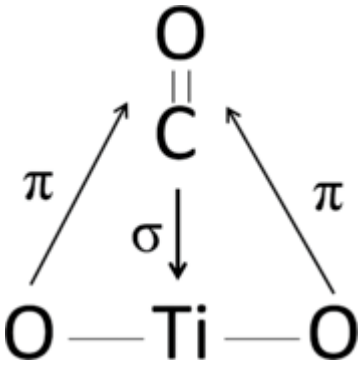

Scheme 1.

σ and π contributions to the CO–TiO_2 interaction. The arrows indicate the direction of electron density donation. The standard through-bond CO→Ti σ-donation is accompanied by π-backdonation from the neighboring surface oxygen anions (which are not bonded to CO).

In summary, the CO–anatase TiO_2 interaction is: 1) synergic—the greater the σ-donation to Ti, the stronger the π-backdonation to CO, 2) facet-specific—its extent depends on the exposed surface, and 3) collective—the surface is the actual electron donor and, via the oxygen anions of the Ti coordination environment, locally plays the Lewis-base role. As a consequence, TiO_2 reactivity, dominated by the Lewis acidity of unsaturated Ti sites, might also be tuned by the Lewis basicity of the top-layer oxygen atoms.

Acknowledgements

The authors acknowledge FAR Insubria 2014 and FP7 SETNanoMetro project (no. 604577) for funding.

Ancillary

Supporting Information

As a service to our authors and readers, this journal provides supporting information supplied by the authors. Such materials are peer reviewed and may be re-organized for online delivery, but are not copy-edited or typeset. Technical support issues arising from supporting information (other than missing files) should be addressed to the authors.

Please note: Wiley-Blackwell is not responsible for the content or functionality of any supporting information supplied by the authors. Any queries (other than missing content) should be directed to the corresponding author for the article.

- 1a*U. Diebold, Surf. Sci. Rep. 2003, 48, 53;*
- 1b*W. Q. Fang, X.-Q. Gong, H. G. Yang, J. Phys. Chem. Lett. 2011, 2, 725;*
- 1c*G. Liu, H. G. Yang, J. Pan, Y. Q. Yang, G. Q. Lu, H.-M. Cheng, Chem. Rev. 2014, 114, 9559;*
- 1d*L. Sang, Y. Zhao, C. Burda, Chem. Rev. 2014, 114, 9283;*
- 1e*N. Sharifi, F. Tajabadi, N. Taghavinia, ChemPhysChem 2014, 15, 3902;*
- 1f*X. Yu, B. Jeon, Y. K. Kim, ACS Catal. 2015, 5, 3316;*
- 1g*M. Yoshii, H. Kobayashi, H. Tada, ChemPhysChem 2015, 16, 1846;*
- 1h*C. Li, C. Koenigsmann, W. Ding, B. Rudshteyn, K. R. Yang, K. P. Regan, S. J. Konezny, V. S. Batista, G. W. Brudvig, C. A. Schmuttenmaer, J.-H. Kim, J. Am. Chem. Soc. 2015, 137, 1520;*
- 1i*L. Liu, Y. Jiang, H. Zhao, J. Chen, J. Cheng, K. Yang, Y. Li, ACS Catal. 2016, 6, 1097.*
- 2*M. Setvin, X. Hao, B. Daniel, J. Pavelec, Z. Novotny, G. S. Parkinson, M. Schmid, G. Kresse, C. Franchini, U. Diebold, Angew. Chem. Int. Ed. 2014, 53, 4714;*
- 3*X.-Q. Gong, A. Selloni, M. Batzill, U. Diebold, Nat. Mater. 2006, 5, 665.*
- 4*R. Hoffmann, Rev. Mod. Phys. 1988, 60, 601.*
- 5*R. P. Eischens, W. A. Pliskin, Adv. Catal. 1958, 10, 1.*
- 6a*M. Xu, H. Noei, K. Fink, M. Muhler, Y. Wang, C. Wöll, Angew. Chem. Int. Ed. 2012, 51, 4731;*
- 6b*M. Setvin, M. Buchholz, W. Hou, C. Zhang, B. Stöger, J. Hulva, T. Simschitz, X. Shi, J. Pavelec, G. S. Parkinson, M. Xu, Y. Wang, M. Schmid, C. Wöll, A. Selloni, U. Diebold, J. Phys. Chem. C 2015, 119, 21044;*
- 6c*N. G. Petrik, G. A. Kimmel, J. Phys. Chem. Lett. 2012, 3, 3425;*
- 6d*P. G. Lustemberg, D. A. Scherlis, J. Chem. Phys. 2013, 138, 124702;*
- 6e*F. Zaera, Chem. Soc. Rev. 2014, 43, 7624;*
- 6f*S. Hu, Z. Wang, A. Mattsson, L. Österlund, K. Hermansson, J. Phys. Chem. C 2015, 119, 5403;*
- 6g*S. Tosoni, H.-Y. T. Chen, G. Pacchioni, ChemPhysChem 2015, 16, 3642;*
- 6h*H.-Y. T. Chen, S. Tosoni, G. Pacchioni, Surf. Sci.* ***2016****, doi:10.1016/j.susc.2016.02.008.*
- 7*G. Blyholder, J. Phys. Chem. 1964, 68, 2772.*
- 8a*P. S. Bagus, K. Hermann, W. Müller, C. J. Nelin, Phys. Rev. Lett. 1986, 57, 1496;*
- 8b*G. Pacchioni, G. Cogliandro, P. S. Bagus, Surf. Sci. 1991, 255, 344;*
- 8c*G. Pacchioni, A. M. Ferrari, P. S. Bagus, Surf. Sci. 1996, 350, 159.*
- 9*K. I. Hadjiivanov, G. N. Vayssilov, Adv. Catal. 2002, 47, 307.*
- 10*M. Casarin, C. Maccato, A. Vittadini, J. Phys. Chem. B 1998, 102, 10745.*
- 11a*C. Lamberti, A. Zecchina, E. Groppo, S. Bordiga, Chem. Soc. Rev. 2010, 39, 4951, and references therein;*
- 11b*D. A. Panayotov, S. Burrows, M. Mihaylov, K. Hadjiivanov, B. M. Tissue, J. R. Morris, Langmuir 2010, 26, 8106;*
- 11c*L. Mino, A. M. Ferrari, V. Lacivita, G. Spoto, S. Bordiga, A. Zecchina, J. Phys. Chem. C 2011, 115, 7694;*
- 11d*L. Mino, G. Spoto, S. Bordiga, A. Zecchina, J. Phys. Chem. C 2012, 116, 17008;*
- 11e*L. Mino, G. Spoto, S. Bordiga, A. Zecchina, J. Phys. Chem. C 2013, 117, 11186.*
- 12*A. G. Pelmenschikov, G. Morosi, A. Gamba, S. Coluccia, J. Phys. Chem. 1995, 99, 15018.*
- 13*R. Soave, G. Pacchioni, Chem. Phys. Lett. 2000, 320, 345.*
- 14*T. Onfroy, W.-C. Li, F. Schüth, H. Knözinger, Phys. Chem. Chem. Phys. 2009, 11, 3671.*
- 15*V. Bolis, C. Morterra, B. Fubini, P. Ugliengo, E. Garrone, Langmuir 1993, 9, 1521.*

- 16*G. Busca, H. Saussey, O. Saur, J. C. Lavalley, V. Lorenzelli, Appl. Catal. 1985, 14, 245.*
- 17*K. I. Hadjiivanov, D. G. Klissurski, Chem. Soc. Rev. 1996, 25, 61*.
- 18a*H. Metiu, S. Chrétien, Z. Hu, B. Li, X. Y. Sun, J. Phys. Chem. C 2012, 116, 10439;*
- 18b*G. Pacchioni, H. J. Freund, Chem. Rev. 2013, 113, 4035.*
- 19*A. A. Tsyganenko, L. A. Denisienko, S. M. Zverev, V. N. Filimonov, J. Catal. 1985, 94, 10.*
- 20a*C. Deiana, M. Minella, G. Tabacchi, V. Maurino, E. Fois, G. Martra, Phys. Chem. Chem. Phys. 2013, 15, 307;*
- 20b*C. Deiana, G. Tabacchi, V. Maurino, S. Coluccia, G. Martra, E. Fois, Phys. Chem. Chem. Phys. 2013, 15, 13391.*
- 21*CPMD 3.17.1, IBM Corp.* ***1990****–****2015*** *and MPI für Festkörperforschung Stuttgart* ***1997****–****2001*** *(www.cpmd.org).*
- 22*M. Farnesi Camellone, J. Zhao, L. Jin, Y. Wang, M. Muhler, D. Marx Angew. Chem. Int. Ed. 2013, 52, 5780; Angew. Chem. 2013, 125, 5892.*
- 23*W. Fang, W. Liu, X. Guo, X. Lu, L. Lu, J. Phys. Chem. C 2011, 115, 8622.*